CHEMISTRY
A EUROPEAN JOURNAL

ChemPubSoc
Europe

DOI: 10.1002/chem.201202832

From Graftable Biphotonic Chromophores to Water-Soluble Organic Nanodots for Biophotonics: The Importance of Environmental Effects

Cédric Rouxel,[b] Marina Charlot,[b] Olivier Mongin,[b, d] Tathavarathy Rama Krishna,[c] Anne-Marie Caminade,[c] Jean-Pierre Majoral,[c] and Mireille Blanchard-Desce*[a, b]

Abstract: The photophysical and two-photon absorption (TPA) properties of biphotonic chromophores with one or two phenol pendant units were studied and compared with that of a model biphotonic quadrupolar chromophore. A water-soluble dendritic structure was then synthesized by using the pendant moieties as starting points for the construction of dendritic branches. We show that the polarity of the environment significantly modulates both the fluorescence and the TPA responses of the different chromophoric derivatives. This extends to more subtle effects that involve phenol pendant moieties that were found to act as discrete solvating units and to modify both the photophysics and the TPA response of the chromophore. This demonstrates the high sensitivity of the TPA response of quadrupolar derivatives to minute alterations in the environment. Moreover, the dendritic branches were found to behave as a peculiar cybotactic environment that was able to tune the fluorescence and TPA response of the inner chromophore by creating a polar environment. This reveals a new direction for exploiting such effects by playing on the dendritic architecture (e.g., the nature and shape of the building blocks, the geometry and position of the chromophore) to modulate the TPA responses.

Keywords: absorption · chromophores · cross-coupling · dendrimers · fluorescence

Introduction

Multiphotonics has gained considerable popularity in recent years in the biology community owing to the many advantages it offers for bioimaging,[1] photodynamic therapy,[2] or control and investigation of biological processes.[3] The use of multiphotonics (i.e., two- or three-photon) excitation as opposed to standard one-photon activation allows one to address femtoliter volumes with 3D resolution while going deeper into tissues by operating with red-near infrared (NIR) excitation wavelengths (thus leading to reduced scattering) instead of UV/blue-visible one-photon excitation. Multiphotonic excitation, however, requires the use of short-pulse lasers as well as chromophores with reasonable two-photon absorption (TPA) cross-sections. In particular, chromophores with a much larger TPA cross-section (σ_2) than endogenous chromophores (determined by Webb and collaborators to be lower or much lower than 1 GM)[4] are beneficial to ensure both selective and efficient photoexcitation. However, the most popular chromophores and fluorochromes used in biology do not show large TPA cross-sections.[5] This has triggered continuous efforts in the last decade to engineer biphotonic chromophores with large TPA cross-sections for various applications.[6] Water-soluble chromophores that combine a large TPA cross-section in the biological spectral window (700–1100 nm) as well as a large fluorescence quantum yield (Φ), photostability, and reduced toxicity are of particular interest for bioimaging and biomedical applications.

In this framework, we have developed a promising route on the basis of the covalent embedding of a defined number of lipophilic biphotonic chromophores within nontoxic and biocompatible dendrimeric architectures. This route led to soft "brilliant" all-organic nano-objects (organic nanodots, or ONDs) that can overcome quantum dots in terms of both one ($\varepsilon\Phi$) and two-photon brilliance ($\sigma_2\Phi$) by several orders of magnitude depending on the number of confined chromophores.[7] Water-soluble monochromophoric organic nanodots in which core biphotonic chromophores are embedded into the dendritic architecture were also developed. These

[a] Dr. M. Blanchard-Desce
Université de Bordeaux
Institut des Sciences Moléculaires (UMR CNRS 5255)
351 Cours de la Libération, 33405 Talence Cedex (France)
Fax: (+33) 540006994
E-mail: m.blanchard-desce@ism.u-bordeaux1.fr

[b] Dr. C. Rouxel, Dr. M. Charlot, Dr. O. Mongin, Dr. M. Blanchard-Desce
Chimie et Photonique Moléculaires, CNRS UMR 6510
Université de Rennes 1
Campus de Beaulieu, 35042 Rennes Cedex (France)

[c] Dr. T. R. Krishna, Dr. A.-M. Caminade, Dr. J.-P. Majoral
Laboratoire de Chimie de Coordination, CNRS
205 route de Narbonne, BP 44099
31077 Toulouse Cedex 4 (France)

[d] Dr. O. Mongin
Institut des Sciences Chimiques de Rennes
CNRS UMR 6226, Université de Rennes 1
Campus de Beaulieu, 35042 Rennes Cedex (France)

Supporting information for this article is available on the WWW under http://dx.doi.org/10.1002/chem.201202832.

biocompatible ONDs are of particular interest as contrast agent tracers for in vivo multiphotonic imaging.[8] These proof of concept water-soluble monochromophoric ONDs were built from a bis-acceptor quadrupolar biphotonic chromophore with a TPA cross-section of 100 GM. To achieve a larger TPA cross-section, we decided to shift to an analogous bis-donor quadrupolar biphotonic chromophore, the TPA cross-section of which has been shown to be significantly larger.[7d,9] Following this aim, a symmetrically functionalized quadrupolar chromophore with two phenol pendant moieties (**3**) for incorporation into the core of the dendritic architecture was synthesized in parallel to its dissymmetrical analogue (**2**) that bears only one phenol pendant moiety, which was used as a decorating biphotonic chromophore for the elaboration of superbrilliant nanodots.[7a,c] The photophysical properties (including the TPA) of biphotonic chomophore **3** were studied and compared with that of a model lipophilic biphotonic chromophore **1**, the photoluminescence properties of which depend significantly on the environment, thus making it a sensitive probe in response to its local environment. Water-soluble dendritic OND **4** was then synthesized from chromophore **3**. Its photophysical properties were investigated and showed that chromophore **1** embedded in the dendritic shell experiences a polar environment that strongly affects its photoluminescence properties. We hereafter describe in detail the synthesis and photophysical properties of the series of compounds and take note of the variation from the model compound, the graftable chromophores, and finally the water-soluble OND. We demonstrate that the environment significantly modulates the TPA responses as shown by polarity-dependent measurements conducted on the model chromophore. This extends to more subtle effects that involve appendices, covalently linked to the chromophores, which act as discrete solvating units with reduced mobility (and thus restricted reorientation). This opens a new path for exploiting such effects by playing on the dendritic architecture to modulate the TPA responses.

Results and Discussion

Synthesis

*Synthesis of model chromophore **1** and functionalized chromophores **2** and **3***: Fluorophores **1**–**3** were prepared by means of Sonogashira cross-coupling reactions. Three different synthetic pathways, direct or stepwise, were explored. Along the first route (Scheme 1), diiodofluorene core **5a**[10] was treated with either trimethylsilylacetylene or 2-methyl-3-butyn-2-ol under palladium(II)-catalyzed conditions to afford **5b** and **5c**, respectively, the deprotection of which gave bis(alkyne) fluorene core **6**. Double Sonogashira coupling of **6** with one equivalent of both iodo derivatives **7**[11] and **8** simultaneously afforded fluorophores **1**, **2**, and **3** in a single-step one-pot reaction. However, this attractive method suffers from a major drawback: the purification is very tedious and initially requires column chromatography to separate three main fractions that contain **1**, **2**, and **3**, respectively. To reach the purity criteria required for fluores-

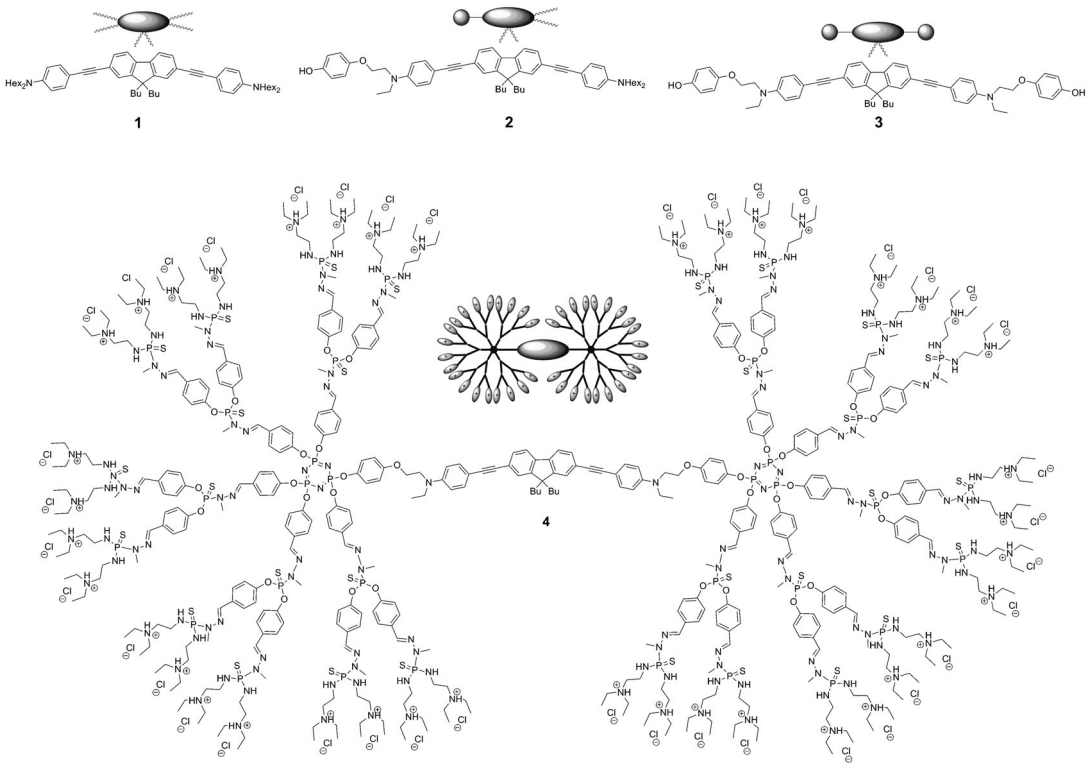

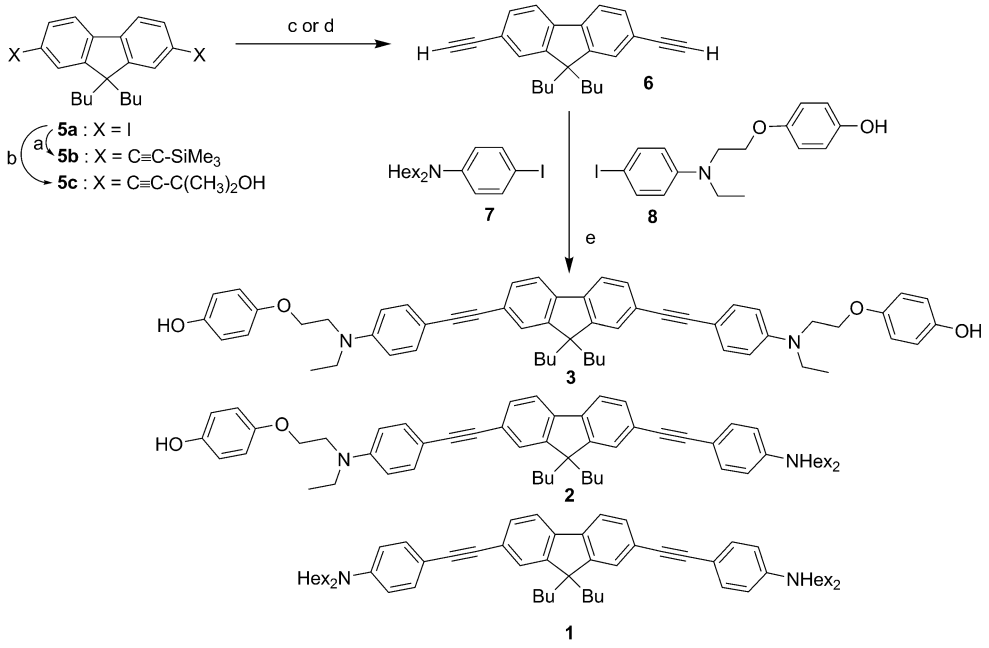

Scheme 1. a) Ethynyltrimethylsilane, $[Pd(PPh_3)_2Cl_2]$, CuI, toluene/Et_3N, 40 °C, 16 h (88 %); b) 2-methyl-3-butyn-2-ol, conditions as in (a), (87 %); c) NaOH, toluene/*i*PrOH, reflux, 30 min (63 %); d) KOH (1 M), THF/MeOH, 20 °C, 15 min (94 %); e) $[Pd(PPh_3)_2Cl_2]$, CuI, toluene/Et_3N, 40 °C, 15 h (4 % of **1**, 6 % of **2**, 5 % of **3**).

cence measurements, each fraction had then to be purified by medium-pressure liquid chromatography (MPLC) by using 20–40 μm silica gel to separate the expected fluorophores from numerous fluorescent byproducts, thus leading to very low isolated yields of 4, 6, and 5 %, respectively (Scheme 1). A possible explanation for the presence of such fluorescent impurities could be related to the oxidation of bis(alkyne) core **6**, thereby resulting in diyne oligomers, the terminal true acetylene functions of which could also react with iodo derivatives **7** and **8**. The use of copper-free conditions and replacing palladium(II) by palladium(0) was unsuccessful and led to an absence of reaction when $[Pd(PPh_3)_4]$ was used. This direct route could therefore not be used for the gram-scale preparation of the target chromophores.

A second route was then investigated for the synthesis of dissymmetric fluorophore **2** on the basis of stepwise functionalization of the fluorene bis(alkyne) core (Scheme 2). Dissymmetrization of core **5c** was performed by deprotecting one of two acetylene protective groups in 44 % yield (but the reaction kinetics were found to be somewhat difficult to control, thereby generating difficulties in reproduction). Sonogashira coupling of **9** with iodo derivative **7** led to **10a** in disappointing 37 % yield, which could not be im-

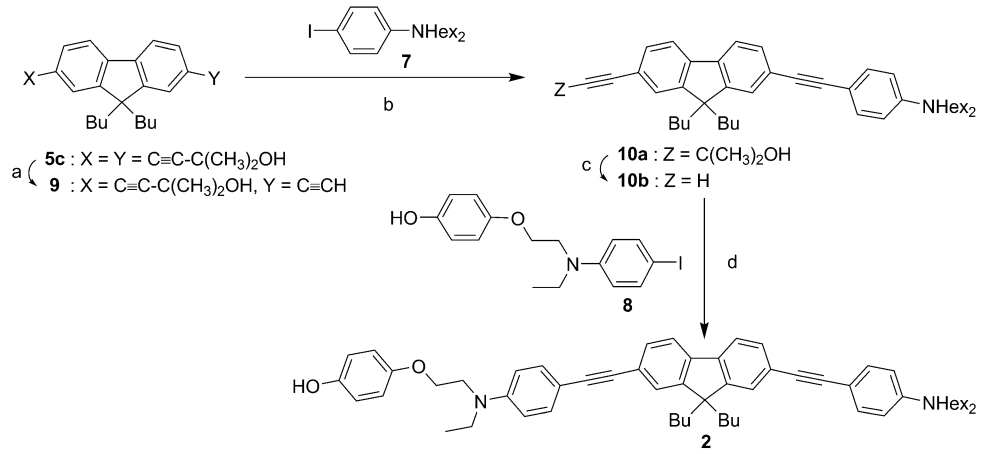

Scheme 2. a) NaOH, toluene/*i*PrOH, reflux (44 %); b) $[Pd(PPh_3)_2Cl_2]$, CuI, toluene/Et_3N, 40 °C, 3.5 h (37 %); c) KOH, toluene/*i*PrOH, reflux, 1 h (87 %); d) $[Pd(PPh_3)_2Cl_2]$, CuI, toluene/Et_3N, 40 °C, 16 h (57 %).

proved by varying catalysts, solvents, or concentrations. Base-promoted deprotection of **10a** afforded **10b** in good yield. Its cross-coupling with the second iodo derivative **8** finally led to fluorophore **2** in moderate 57% yield (Scheme 2). The major advantage of this second route is that purifications are much easier than for the first route; however, the overall yield of this four-step sequence (8%) remained unsatisfactory.

The third route is based on the stepwise functionalization of a diiodo fluorene core with two acetylenic moieties obtained from the corresponding iodo derivatives **7** and **8** (Scheme 3 and 4). Building block **7**[11] was treated with either ethynyltrimethylsilane or 2-methyl-3-butyn-2-ol to afford **11a**[12] and **11b**, respectively, and base-promoted deprotection of the latter gave **12**.[9c] On the other hand, iodo derivative **8** (obtained from the Mitsunobu reaction between **13**[13] and hydroquinone) was also treated with ethynyltrimethylsilane to afford **14a** in mediocre 45% yield. Cleavage of the trimethylsilyl group led to **14b** in a very low isolated yield (most probably due to degradation during the purification). To check whether the large difference in yield between **11a** and **14a** could be related to the presence of the phenol function, compound **8** was esterified with acetyl chloride. The cross-coupling of resulting compound **15a** with ethynyltrimethylsilane afforded **15b** in a notably increased 81% yield. However, cleavage of the silyl protective group gave **15c** in a better but still unsatisfactory 45% yield (Scheme 3).

If degradation during the purification is indeed the explanation, **15c** should not be isolated, but generated in situ from **15b** during the Sonogashira couplings. In a one-pot reaction, **15b** was therefore deprotected with tetra-*n*-butylammonium fluoride (TBAF), and the liberated alkyne was treated with diiodo fluorene core **5a** in the presence of palladium(II) and copper(I) in toluene/Et_3N, thus leading to dissymmetrized molecule **16**. The concomitant formation of the double coupling product was limited by using an excess amount of the diiodo core (which could easily be recycled). It should be noticed that, under the same conditions, cross-coupling of **11a** (or **12**) with **5a** did not proceed. In contrast, compound **17** was obtained by reaction of **11a** with **16** in a satisfactory 75% yield. Saponification of acetate protective groups of **17** with diluted NaOH afforded fluorophore **2**. The overall yield of this three-step sequence is 37%, which allowed for gram-scale preparation of **2** (Scheme 4).

Symmetrical fluorophore **3** could be obtained similarly in a two-step sequence from diodo core **5a**. Double Sonogashira coupling of **5a** with **15b** (deprotected in situ with TBAF) led efficiently to **18**, the saponification of which afforded **3** (Scheme 5). However, the synthesis of fluorophore **1** by reaction between **5a** and **11a** or **12** failed under these conditions and no coupling occurs. Among attempts to increase reactivity, the replacement of toluene with THF was found to give **1** in fair yield (Scheme 5).

*Synthesis of water-soluble organic dendrimer **4***: Fluorophore **3**, which bears two phenol groups, was used as the core of the water-soluble dendrimer **4**. The first reaction is the coupling with hexachlorocyclotriphosphazene ($N_3P_3Cl_6$), which was used in a large excess amount to favor the monosubstitution reaction. Compound **19** was isolated in very good

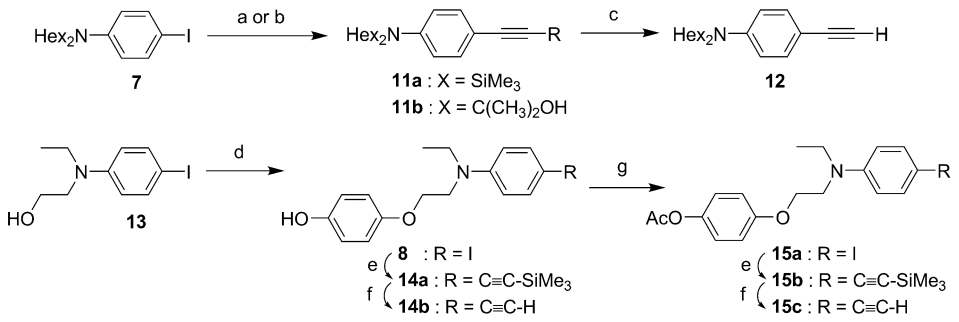

Scheme 3. a) Ethynyltrimethylsilane, $[Pd(PPh_3)_2Cl_2]$, CuI, toluene/Et_3N, 40°C, 18 h (90%); b) 2-methyl-3-butyn-2-ol, conditions as in (a) (82%); c) NaOH, toluene/*i*PrOH, reflux, 1 h (87%); d) hydroquinone, diethyl azodicarboxylate (DEAD), PPh_3, THF, 20°C, 16 h (51%); e) $[Pd(PPh_3)_2Cl_2]$, CuI, toluene/Et_3N, 40°C, 15 h (45% of **14a**, 81% of **15b**); f) THF, TBAF, 20°C, 15 min (12% of **14b**, 45% of **15c**); g) acetyl chloride, DMAP, CH_2Cl_2/Et_3N, 20°C, 14 h (76%).

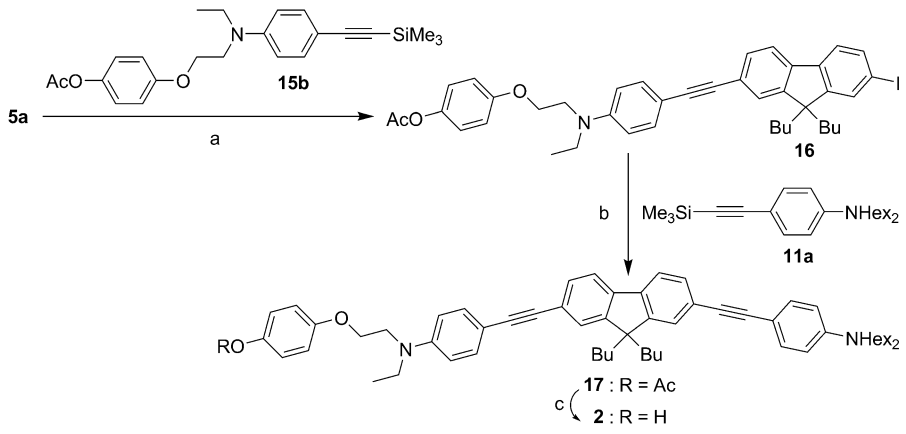

Scheme 4. a) Compound **5a** (3 equiv), **15b** (1 equiv), TBAF, $[Pd(PPh_3)_2Cl_2]$, CuI, toluene/Et_3N, 40°C, 15 h (54%); b) TBAF, $[Pd(PPh_3)_2Cl_2]$, CuI, toluene/Et_3N, 40°C, 15 h (75%); c) NaOH (0.5 M), THF, EtOH, 20°C, 15 min (91%).

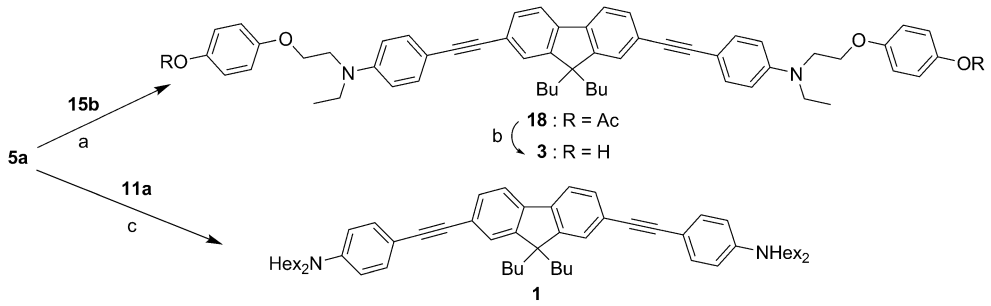

Scheme 5. a) TBAF, $[Pd(PPh_3)_2Cl_2]$, CuI, toluene/Et_3N, 40 °C, 16 h (76 %); b) NaOH (0.5 M), THF/EtOH, 20 °C, 25 min (98 %); c) $[Pd(PPh_3)_2Cl_2]$, CuI, THF/Et_3N, TBAF, 50 °C, 16 h (59 %).

yield (93 %). The nonsymmetric functionalization of $N_3P_3Cl_6$ was demonstrated by the ^{31}P NMR spectra in particular, which display the presence of two signals, one of which resembled a triplet at $\delta = 13.0$ ppm, which corresponds to the phosphorus atom that bears the chromophore, and the other one of which resembled a doublet at $\delta = 22.4$ ppm, which corresponds to both PCl_2 groups, with $^2J(P,P) = 59.2$ Hz.

The growth of the branches was then carried out by using our classical method of dendrimer synthesis.[14] The first step of the growth is the nucleophilic substitution of Cl by 4-hydroxybenzaldehyde, which affords dendrimer **20**, characterized by ^{31}P NMR spectroscopy by the disappearance of the doublet and triplet of **19** on behalf of a complex system at $\delta = 7.2$–7.9 ppm for **20**. The second step of the growth is the condensation reaction of the aldehydes of **20** with the phosphorhydrazide $H_2NN(Me)P(S)Cl_2$, which affords dendrimer **21**. The completion of the reaction is characterized by the total disappearance of the signals that correspond to the aldehydes in the ^1H NMR spectra. The growth of the dendrimer is pursued by repeating the first step (i.e., the substitution reaction with 4-hydroxybenzaldehyde), thus leading to dendrimer **22**. The repetition of the second step (i.e., the condensation with the phosphorhydrazide) affords dendrimer **23**. All these reactions are quantitative, thus all the dendrimers are isolated in excellent yields after workup.

To have a water-soluble dendrimer, the terminal groups must bear charges. We chose to graft ammonium groups by treating them with *N*,*N*-diethylethylenediamine.[15] The reaction of the NH_2 side with $P(S)Cl_2$ terminal groups of the dendrimer generates HCl, which is trapped by the NEt_2 side, thereby affording water-soluble and multi-charged dendrimer **4**. The completion of the reaction is shown in the ^{31}P NMR spectra by the disappearance of the singlet that corresponded to $P(S)Cl_2$ groups at $\delta = 62.8$ ppm on behalf of a singlet at $\delta = 69.8$ ppm, which corresponded to $P(S)(NHR)_2$ (Scheme 6).

Photophysical properties

*Absorption and fluorescence of chromophores **1**–**3**: Structural effects*: The photophysical properties of chromophores **1**–**3** are collected in Table 1. All chromophores strongly absorb in the near-UV region and show attractive photoluminescence properties with large fluorescence quantum yields in organic solvents. As illustrated in Figure 1, we observed that the presence of phenol pendant moieties leads to a slight but yet observable modification of absorption and emission spectra, thus indicating that those end groups slightly modify the environment. A slight blueshift of both absorption and emission spectra is observed with the addition of pendant phenol moieties. In addition, a clear change of vibronic structure is observed upon going from chromophore **1** to **3** with a relative rise of the 01 and 02 vibronic substructure with respect to that of the 00 one. This effect, which reveals an increase in reorganization energy,[16] indicates that the alkyloxyphenol moieties act as discrete "solvating" molecules that contribute to solvent reorganization in the excited state. This is consistent with a regular increase of the Stokes shift values with an increased number of appending moieties (i.e., from **1** to **3**).

The presence of pendant moieties also induces a slight broadening of the absorption band (consistent with a lower extinction coefficient at absorption maximum), which might be attributed to an increase in inhomogeneous broadening caused by the proximity of alkyloxyphenol moieties that are connected by means of flexible spacers, thus generating a distribution of conformations. We also observe that the phenol moieties cause a decrease in the fluorescence quantum yield as well as of the fluorescence lifetime. The shorter radiative lifetime can be related to a slight increase in radiative decay rate (in relation with the blueshifted emission and the enhancement of oscillatory force[17]) and a marked increase in the nonradiative decay rate. This marked increase (by a factor larger than two for symmetrical chromophore **3** relative to chromophore **1**, which lacks the phenol terminal moieties) suggests that phenol moieties are involved in additional nonradiative decay channels. These most probably involve hydrogen bonds with surrounding solvent molecules that promote vibrational deactivation and are therefore responsible for the decrease in fluorescence quantum yield.

*Influence of environment on the photophysical properties of chromophores **1**–**3***: The influence of environmental effects was checked by investigating the absorption and emission properties of chromophore **3** in solvents of varying polarities

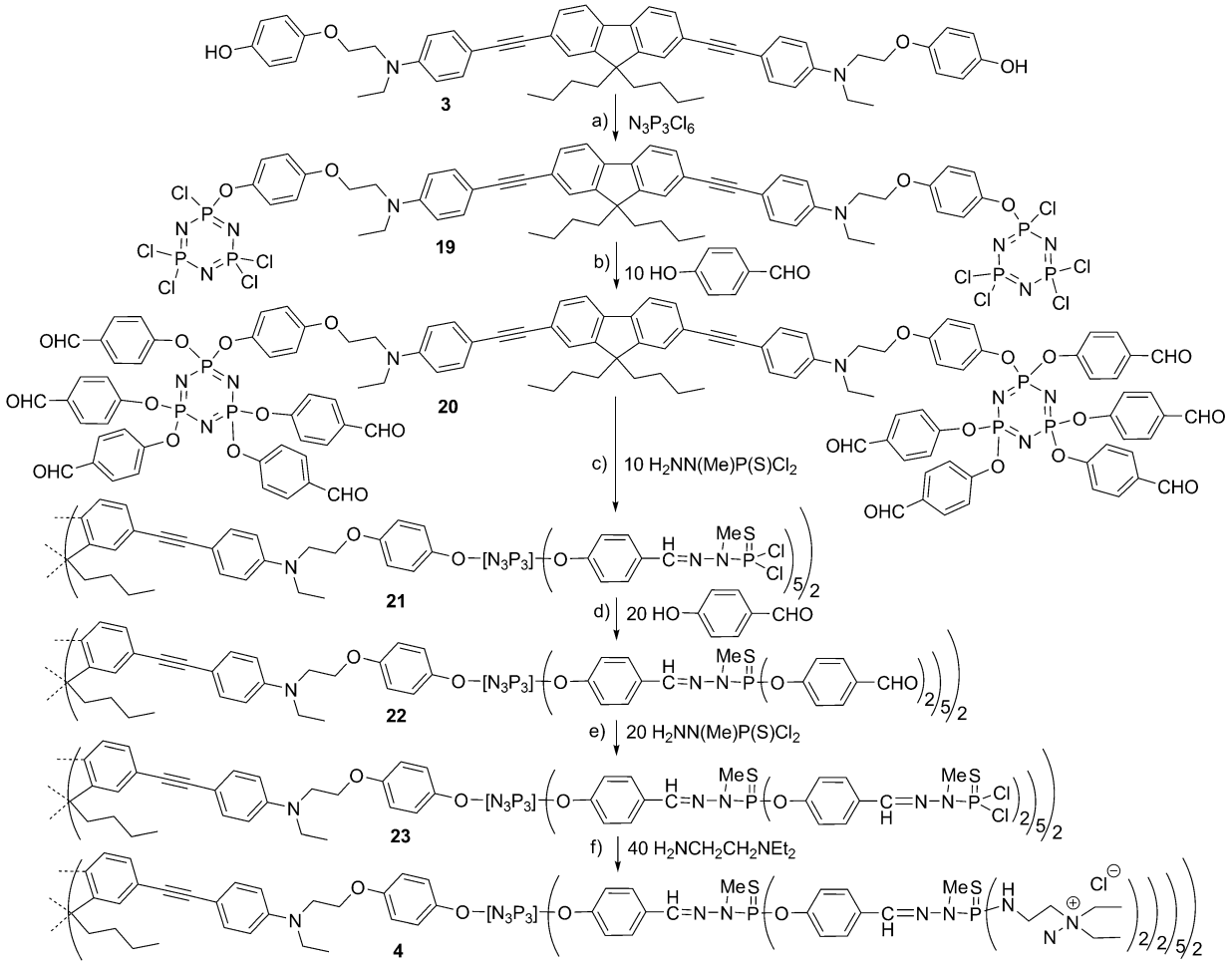

Scheme 6. a) TBAF, $[Pd(PPh_3)_2Cl_2]$, CuI, toluene/Et_3N, 40 °C, 16 h (76 %); b) NaOH (0.5 M), THF/EtOH, 20 °C, 25 min (98 %); c) $[Pd(PPh_3)_2Cl_2]$, CuI, THF/Et_3N, TBAF, 50 °C, 16 h (59 %).

(Table 2). As shown in Figure 2, chromophore **3** absorption spectra are only weakly affected by solvent polarity (except for a high-polarity solvent like DMSO, which leads to a slight redshift as well as a broadening of the absorption band). In contrast, its emission is strongly dependent on solvent polarity, which shifts from the violet to the blue-green region upon going from low-polarity to high-polarity solvents. As a consequence, chromophore **3** behaves like a sensitive fluorescent probe toward its environment. A similar behavior is observed for chromophores **1**[18] and **2** (see the Supporting Information). As shown in Figure 3, the solvatochromic behavior of each compound in solvents of medium to high polarity can be fit with a Lippert–Mataga relationship in which the Stokes shift values are linearly correlated to the polarity/polarizability function of the solvent Δf [Eq. (1)]:[19]

$$\tilde{\nu}_{abs} - \tilde{\nu}_{em} = 2\Delta\mu^2\Delta f/(hca^3) + \text{constant} \quad (1)$$

in which $\tilde{\nu}_{abs}$ ($\tilde{\nu}_{em}$) is the wavenumber of the absorption (fluorescence) maximum, h is the Planck constant, c is the light velocity, a is the radius of the solute spherical cavity, and $\Delta f = (\varepsilon-1)/(2\varepsilon+1) - (n^2-1)/(2n^2+1)$, in which ε is the dielectric constant and n the refractive index of the solvent.

Table 1. Photophysical data for compounds **1**–**3** in toluene.

Compound	λ_{max}^{abs} [a] [nm]	ε [b] [$M^{-1}cm^{-1}$]	FWHM [cm^{-1}]	f [c]	λ_{max}^{em} [d] [nm]	Stokes shift [cm^{-1}]	Φ [e]	τ [f] [ns]	k_r [g] [10^9 s^{-1}]	k_{nr} [g] [10^9 s^{-1}]	τ_0 [h] [ns]	r [i]
1	388	85800	4190	1.4	422, 445	2080	0.87	0.74	1.18	0.17	0.85	0.18
2	386	84900	4330	1.5	420, 444	2100	0.83	0.67	1.24	0.25	0.81	0.18
3	381	83800	4640	1.6	418, 440	2320	0.77	0.55	1.40	0.42	0.71	0.18

[a] Experimental absorption maxima. [b] Molar extinction coefficient. [c] Oscillator strength. [d] Experimental emission maximum. [e] Fluorescence quantum yield determined in chloroform relative to quinine in 0.5 M H_2SO_4. [f] Experimental fluorescence lifetime. [g] Radiative (k_r) and nonradiative (k_{nr}) decay rates. [h] Radiative lifetime. [i] Fluorescence anisotropy.

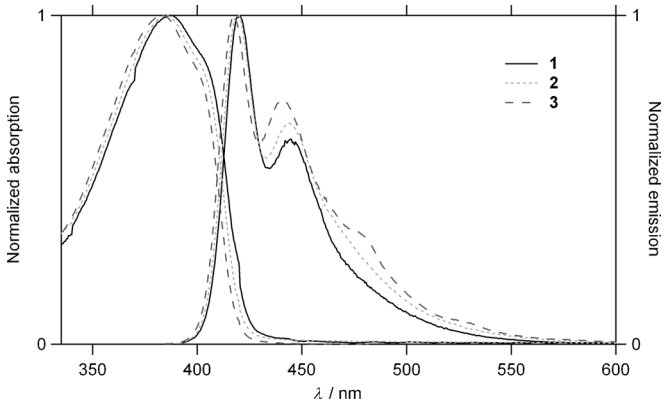

Figure 1. Normalized absorption and emission spectra of chromophores **1**–**3** in toluene.

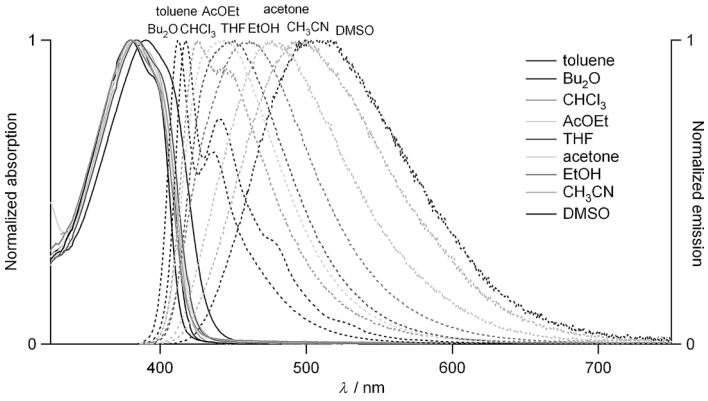

Figure 2. Normalized absorption and emission spectra of chromophore **3** in solvents of different polarity.

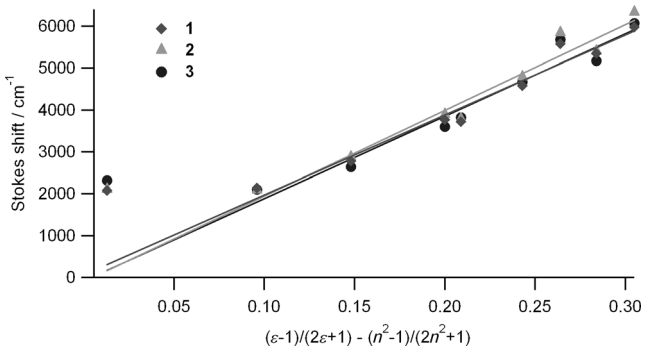

Figure 3. Lippert–Mataga correlations for fluorophores **1**–**3**.

Such behavior can be related to a symmetry breakage that occurs in the excited state of the quadrupolar donor–acceptor–donor (DAD) compound, which leads to localization of the excitation on a dipolar chromophoric subunit (donor–acceptor, or DA).[19b] Hence the emission behavior is similar to that of push/pull chromophores and shows intramolecular charge transfer (ICT) with an increase in the dipole moment in the excited state. We note that the Stokes shift values in low-polarity solvent (i.e., toluene) always stand out from the linear correlation. This reveals that symmetry breakage occurs only in medium- to high-polarity solvents, thanks to the stabilization of the corresponding excited state provided by such solvents.[20] This explains the higher radiative decay rate measured in toluene (relative to dibutyletheroxide) on account of the extended delocalization in the emissive excited state only in toluene.

The slopes values derived from the Lippert–Mataga relationship (i.e., $2\Delta\mu^2/hca^3$, also termed specific shifts[21]), which are directly related to the magnitude of the photoinduced intramolecular charge transfer ($\Delta\mu$) and to the size of the Onsager cavity (a), are collected in Table 3. To obtain information on the size of the molecule, we used fluorescence anisotropy (r) and lifetime (τ) data in DMSO to calculate the longitudinal rotational correlation time (θ) by using the Perrin equation [Eq. (2)]:[22]

Table 3. Solvatochromic and anisotropy data for chromophores **1**–**3**.

Compound	Specific shift[a] [10^3 cm^{-1}]	r[b]	τ[c] [ns]	θ[d] [ns]	v[e] [Å^3]	l[f] [Å]	a[g] [Å]	$\Delta\mu$ [D]
1	19.1	0.20	1.92	1.92	7900	12.4	6.2	20.9
2	20.5	0.20	1.96	1.96	8050	12.4	6.2	21.9
3	19.8	0.217	1.46	1.73	7100	11.9	6.0	20.2

[a] Slope derived from the linear dependence of the Stokes shift on the orientational polarizability function Δf. [b] Florescence anisotropy (in DMSO). [c] Fluorescence lifetime (in DMSO). [d] Longitudinal rotational correlation time (in DMSO). [e] Molecular rotor volume. [f] Molecular long axis derived from fluorescence anisotropy. [g] Dipolar Onsager cavity radius

Table 2. Photophysical data of chromophore **3** in different solvents.

Solvent	λ_{max}^{abs} [a] [nm]	ε_{max} [M^{-1}cm^{-1}]	λ_{max}^{em} [b] [nm]	Stokes shift [cm^{-1}]	Φ[c]	τ_f[d] [ns]	τ_0[e] [ns]	k_r[f] [10^9 s^{-1}]	k_{nr}[f] [10^9 s^{-1}]
toluene	381	83800	418, 440	2300	0.77	0.55	0.71	1.40	0.42
Bu_2O	380	82300	413, 436	2100	0.77	0.82	1.06	0.94	0.28
AcOEt	382	88800	443	3600	0.81	1.04	1.28	0.78	0.18
THF	384	83200	450	3800	0.80	1.02	1.28	0.78	0.20
acetone	382	86000	476	5200	0.71	1.36	1.92	0.52	0.21
EtOH	380	84500	462	4700	0.80	1.23	1.54	0.65	0.16
CH_3CN	383	83300	499	6100	0.69	1.65	2.39	0.42	0.19
DMSO	390	86900	501	5700	0.78	1.46	1.87	0.53	0.15

[a] Experimental absorption maxima. [b] Experimental emission maximum. [c] Fluorescence quantum yield determined relative to quinine in 0.5 M H_2SO_4. [d] Experimental fluorescence lifetime. [e] Radiative lifetime. [f] Radiative (k_r) and nonradiative (k_{nr}) decay rates.

$$\theta = \frac{\tau}{(0.4/r) - 1} \quad (2)$$

Assuming a prolate-type behavior,[22] the correlation time (θ) is directly related to the size of the chromophore (molecular rotor long axis l) according to Equation (3):

$$l = \sqrt[3]{\frac{3kT\theta}{4\pi\eta}} \quad (3)$$

in which η is the solvent viscosity.

From the long axis of the molecule derived from fluorescence anisotropy measurements (l), one can derive the radius a of the Onsager cavity for the dipolar subunit.[23] The derived data are gathered in Table 3. The presence of the ethyloxyphenol appendages induces a slight reduction of the $\Delta\mu$ value in the case of symmetrical derivative **3** and a slight increase in the case of asymmetrical derivative **2**. This confirms that the phenol pendant moieties influence the photophysical properties of the core chromophore unit by modifying its cybotactic environment, most probably by means of dipole–dipole interactions that destabilize the polar excited state in the case of chromophore **3** (in agreement with blueshifted emission) but facilitates symmetry breakage in the case of chromophore **2**.

For all chromophores **1**–**3**, we observed that the fluorescence quantum yields remain high in all solvents (0.7–0.8), whereas the fluorescence lifetime increases with increasing polarity. This peculiar behavior can be related to the parallel and steady decrease in both radiative (as expected from the redshifted emission) and nonradiative decay rates with increasing polarity.

*Absorption and fluorescence of water-soluble dendritic compound **4***: The photophysical properties of compound **4** were first studied in DMSO, which was chosen owing to its ability to dissolve both chromophore **3** and its water-soluble dendritic derivative **4** and thus allow direct comparison and assessment of the effect of the dendritic architecture on the photophysical properties of the embedded chromophore. As observed in Table 4, the absorption band of the core chromophore is slightly blueshifted owing to the overlap with the red edge of the dendritic architectures absorption band located in the UV region. We stress that selective one-photon excitation of the inner chromophore is thus effective only above 400 nm. The emission properties of chromophore **4** in DMSO are only slightly different from that of its parent chromophore **3**. The emission band is only slightly blueshifted, which is indicative of a faintly less polar environment (between that of acetonitrile and DMSO) in the core of the dendritic structure relative to the bulk solution. This suggests that DMSO molecules permeate the dendritic architectures, thus leading to an effective polarity close to that of DMSO. We also note that the fluorescence quantum yield is reduced by about half in the dendritic architecture as compared to the bulk solution. This indicates that competitive nonradiative decay processes take place, which possibly involve the dendritic backbone. On the other hand, the fluorescence anisotropy markedly increases from chromophore **3** to dendritic chromophore **4** (thus almost reaching the limit value) as expected on account of the larger size of compound **4**, which leads to much longer rotational correlation time.

Table 4. Fluorescence characteristics of dendritic compound **4**.

Solvent	λ_{max}^{abs} [a] [nm]	λ_{max}^{em} [nm]	Φ	τ_f [ns]	r
4/DMSO	385	487	0.42	1.69 (80%) 0.33 (20%)	0.32
4/H_2O	385	480	0.075	0.70 (70%) 2.39 (30%)	0.096

In contrast to DMSO, the emission characteristics of **4** in water are strongly affected. The absorption band is clearly broadened (in relation to inhomogeneous broadening) and weakened, whereas the emission band is even more blueshifted, which is indicative of a less polar environment than acetone (Figure 4). This indicates that water molecules have much lower affinity for the dendritic structure core (owing to the lipophilic nature of the branches) than DMSO, thereby leading to a less polar environment for the core chromophore. Strikingly, both the fluorescence quantum yield and the anisotropy of dendritic derivative **4** were found to decrease dramatically. This suggests that these dendritic architectures tend to self-assemble in water, thus favoring fast energy transfer between chromophores. The presence of flexible linkers in molecule **3** as well as the elongated rod-like shape and hydrophobic nature of the core chromophore might facilitate the formation of aggregates of dendritic compound **4** in water. Such behavior is consistent with the double-exponential decay of fluorescence. Compared to the results reported earlier for water-soluble dendritic architectures built from a much more compact chromophoric core that lacks flexible linkers,[8] these results indicate that the core chromophore in compound **4** is not sufficiently isolated from the external environment and that better (i.e., tighter)

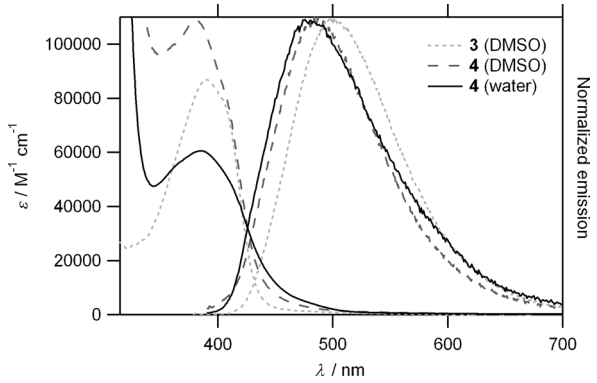

Figure 4. Absorption and emission spectra of dendrimer **4** in DMSO and water relative to those of isolated fluorophore **3** in DMSO.

shielding is needed to prevent self-aggregation and to further enhance the fluorescence emission in water.

Two-photon absorption: Environmental and symmetry effects: To monitor environmental effects on TPA and compare them with one-photon absorption, we first investigated the two-photon properties of core chromophore **3** in solvents of various polarities. The TPA spectra were determined in the NIR range (700–980 nm) by investigating their two-photon excited fluorescence (TPEF) in various solutions.[5] As noted from Figure 5, solvent polarity has much more influence on TPA than on one-photon absorption (see Table 1 and Figure 2) and a non-monotonous variation is obtained. We observed a decrease in the TPA response upon going from low-polarity (e.g., THF) to medium-polarity solvent (e.g., acetone) followed by an increase in polar solvents as well as redshift of the strongly two-photon-allowed absorption band (which lies at higher energy than that which corresponds to the lowest one-photon-allowed excited state, in relation with quadrupolar symmetry).[9c] As a result, the TPA maximum is clearly seen in the 700–750 nm spectral range only in the case of highly polar solvents such as DMSO. This TPA redshift parallels the one-photon absorption redshift observed in DMSO.

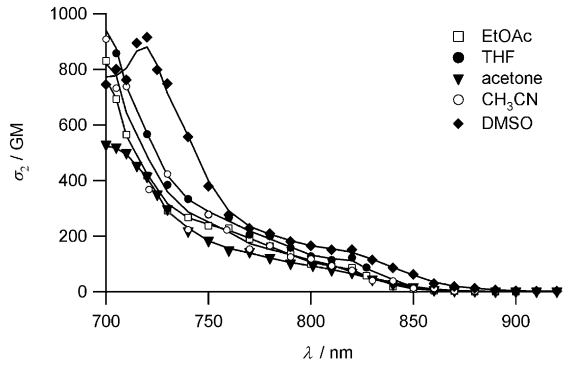

Figure 5. Two-photon absorption spectra of core fluorophore **3** in various solvents.

The TPA properties of dendritic system **4** dissolved in water were found to be between that of chromophore **3** in DMSO and in acetonitrile (Figure 6). This confirms that the dendritic shell provides a polar environment for the core chromophore that affects its TPA response, as is the case for fluorescence.

Interestingly, we observe a marked broadening, particularly in the red-edge region, with the increase in the TPA band that corresponded to the one-photon-allowed, two-photon-forbidden excited state. This effect might be related to the self-association of compound **4** in water, which promotes symmetry breakage.

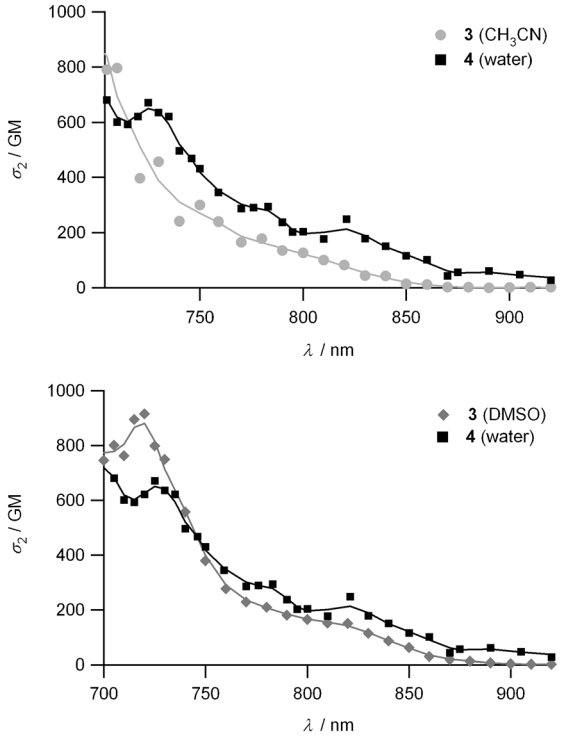

Figure 6. Two-photon absorption spectra of dendrimer **4** in water relative to **3** in acetonitrile and DMSO.

Conclusion

From the present study, we can deduce that not only bulk polarity but also the presence of discrete solvating units (such as ethyloxy phenol moieties) influences the fluorescence and TPA properties of prototypical quadrupolar biphotonic chromophores. As a result, the quadrupolar chromophore embedded at the core of the dendritic structure was found to be sensitive to the particular cybotactic environment provided by the dendritic branches, which creates a local setting that is favorable to TPA. This opens a new direction for engineering the TPA response of biphotonic chromophores by taking advantage of and tuning the dendritic environment. We are currently investigating this route. We are also trying to provide better protection by the dendritic shell to prevent fluorescence quenching and ensure high two-photon brightness in water.

Experimental Section

General synthetic methods: All air- or water-sensitive reactions were carried out under dry argon. Solvents were generally dried and distilled prior to use. Reactions were monitored by thin-layer chromatography on Merck silica gel 60 F_{254} precoated aluminum sheets. For column chromatography, Merck silica gel Si 60 (40–63 μm, 230–400 mesh or 63–200 μm, 70–230 mesh) was used. Melting points were determined using an Electrothermal IA9300 digital melting-point instrument. For NMR spectroscopy, Bruker ARX 200 (^{1}H: 200.13 MHz, ^{13}C: 50.32 MHz) or Avance AV 300 (^{1}H: 300.13 MHz, ^{13}C: 75.48 MHz) instruments were used with

$CDCl_3$ solutions; ^1H chemical shifts (δ) are given in ppm relative to TMS as internal standard, J values in Hz and ^{13}C chemical shifts relative to the central peak of $CDCl_3$ at $\delta = 77.0$ ppm. High- and low-resolution mass spectra measurements were performed at the Centre Régional de Mesures Physiques de l'Ouest (CRMPO, Rennes) using a Micromass MS/MS ZABSpec time-of-flight (TOF) instrument with emitter–base–emitter (EBE) TOF geometry. Liquid secondary ion mass spectrometry (LSIMS) was carried out at 8 kV with Cs^+ in *m*-nitrobenzyl alcohol (*m*NBA); ES^+ (electrospray ionization, positive mode) at 4 kV; electron ionization (EI) at 70 eV. Elemental analyses were performed at CRMPO. Compounds **5a**,[10] **7**,[11] **11b**,[9c] **12**,[9c] and **13**[13] were synthesized according to the respective literature procedures.

Compound 5b: Air was removed from a solution of **5a**[10] (3.00 g, 5.66 mmol) in toluene/Et_3N (5:1; 37.5 mL) by blowing argon for 20 min. Then CuI (21.6 mg, 0.113 mmol), $[Pd(PPh_3)_2Cl_2]$ (79.6 mg, 0.113 mmol), and trimethylsilylacetylene (2.4 mL, 1.67 g, 16.98 mmol) were added, and the mixture was stirred at 40 °C for 16 h. After evaporation of the solvents, the residue was purified by column chromatography (heptane/CH_2Cl_2 90:10) to yield **5b** (2.35 g, 88 %). $R_f = 0.24$ (heptane); ^1H NMR (200.13 MHz, $CDCl_3$): $\delta = 7.64$ (d, $J = 7.5$ Hz, 2H), 7.48 (d, $J = 7.5$ Hz, 2H), 7.46 (s, 2H), 1.98 (m, 4H), 1.08 (m, 4H), 0.69 (t, $J = 7.3$ Hz, 6H), 0.55 (m, 4H), 0.33 ppm (s, 18H); ^{13}C NMR (50.32 MHz, $CDCl_3$): $\delta =$ 150.9, 140.9, 131.3, 126.2, 121.8, 119.9, 106.1, 94.3, 55.2, 40.2, 25.8, 23.1, 13.8, 0.1 ppm; HRMS (EI): m/z calcd for $C_{31}H_{42}Si_2$ [$M^{+\bullet}$]: 470.2825; found: 470.2848; elemental analysis calcd (%) for $C_{31}H_{42}Si_2$ (470.85): C 79.08, H 8.99; found: C 78.88, H 9.12.

Compound 5c: Air was removed from a solution of **5a**[10] (6.00 g, 11.3 mmol) in toluene/Et_3N (5:1, 40 mL) by blowing argon for 20 min. Then CuI (86 mg, 0.45 mmol), $[Pd(PPh_3)_2Cl_2]$ (316 mg, 0.45 mmol), and 2-methyl-3-butyn-2-ol (2.84 g, 33.8 mmol) were added, and the mixture was stirred at 40 °C for 16 h. After evaporation of the solvents, the residue was purified by column chromatography (heptane/CH_2Cl_2 30:70 then CH_2Cl_2) to yield **5c** (4.37 g, 87 %). $R_f = 0.29$ (CH_2Cl_2/AcOEt 95:5); ^1H NMR (200.13 MHz, $CDCl_3$): $\delta = 7.60$ (d, $J = 8.6$ Hz, 2H), 7.40 (d, $J =$ 8.6 Hz, 2H), 7.38 (s, 2H), 2.16 (s, 2H), 1.94 (m, 4H), 1.66 (s, 12H), 1.07 (m, 4H), 0.66 (t, $J = 7.3$, 6H), 0.52 ppm (m, 4H); ^{13}C NMR (50.32 MHz, $CDCl_3$): $\delta = 150.8$, 140.5, 130.7, 126.0, 121.3, 119.8, 93.9, 82.9, 65.7, 55.0, 40.1, 31.5, 25.7, 23.0, 13.8 ppm; HRMS (EI): m/z calcd for $C_{31}H_{38}O_2$ [$M^{+\bullet}$]: 442.2872; found: 442.2859; elemental analysis calcd (%) for $C_{31}H_{38}O_2$ (442.64): C 84.12, H 8.65; found: C 84.01, H 8.71.

Compound 6: *Method A*: Solid NaOH (303 mg, 7.73 mmol) was added to a solution of **5c** (3.322 g, 7.52 mmol) in toluene/isopropanol (3:1, 48 mL) heated to reflux. The mixture was stirred under reflux for 30 min. After cooling, NaOH was removed by filtration and the solvents were evaporated. The crude product was purified by column chromatography (heptane/CH_2Cl_2 90:10) to yield **6** (1.55 g, 63 %). *Method B*: Aqueous KOH (1 M, 30 mL) was added to a solution of **5b** (1.94 g, 4.12 mmol) in THF/MeOH (3:1, 100 mL), and the mixture was stirred at 20 °C for 15 min. After addition of water, extraction with CH_2Cl_2, and drying ($MgSO_4$), the solvents were removed under reduced pressure. The crude product was purified by column chromatography (heptane/CH_2Cl_2 90:10) to yield **6** (1.26 g, 94 %). $R_f = 0.34$ (heptane/CH_2Cl_2 90:10); ^1H NMR (200.13 MHz, $CDCl_3$): $\delta = 7.63$ (d, $J = 8.6$ Hz, 2H), 7.48 (d, $J = 8.6$ Hz, 2H), 7.46 (s, 2H), 3.15 (s, 2H), 1.94 (m, 4H), 1.07 (m, 4H), 0.67 (t, $J = 7.2$ Hz, 6H), 0.54 ppm (m, 4H); ^{13}C NMR (50.32 MHz, $CDCl_3$): $\delta = 151.0$, 140.9, 131.2, 126.5, 120.8, 119.9, 84.5, 77.4, 55.1, 40.0, 25.8, 22.9, 13.7 ppm; HRMS (EI): m/z calcd for $C_{25}H_{26}$ [$M^{+\bullet}$]: 326.2035; found: 326.2036; elemental analysis calcd (%) for $C_{25}H_{26}$ (326.48): C 91.97, H 8.03; found: C 92.17, H 8.07.

Compound 8: A solution of diethyl azodicarboxylate (DEAD; 9.00 g, 51.7 mmol) in THF (40 mL) was added dropwise to a solution of **13**[13] (5.00 g, 17.2 mmol), hydroquinone (5.65 g, 51.3 mmol), and triphenylphosphine (13.50 g, 51.5 mmol) in THF (110 mL). The mixture was stirred at 20 °C for 16 h, and the solvent was removed under reduced pressure. The residue was purified by column chromatography (CH_2Cl_2) to yield **8** (3.35 g, 51 %). $R_f = 0.32$ (CH_2Cl_2); ^1H NMR (200.13 MHz, $CDCl_3$): $\delta = 7.44$ and 6.50 (AA′XX′, J(A,X) = 9.3 Hz, 4H), 6.75 (s, 4H), 4.47 (s, 1H), 4.03 (t, $J = 6.0$ Hz, 2H), 3.65 (t, $J = 6.0$ Hz, 2H), 3.43 (q, $J = 7.0$ Hz, 2H), 1.17 ppm (t, $J = 7.0$ Hz, 3H); ^{13}C NMR (50.32 MHz, $CDCl_3$): $\delta =$ 152.6, 149.6, 147.1, 137.7, 116.1, 115.5, 114.1, 76.5, 65.9, 49.6, 45.5, 12.0 ppm; HRMS (ES^+): m/z calcd for $C_{16}H_{19}INO_2$ [M+H]$^+$: 384.0461; found: 384.0459; elemental analysis calcd (%) for $C_{16}H_{18}INO_2$ (383.23): C 50.15, H 4.73, N 3.65; found: C 50.36, H 4.85, N 3.65.

Compound 9: Solid NaOH (0.73 g) was added to a solution of **5c** (4.02 g, 9.09 mmol) in toluene/*i*PrOH (6:1, 50 mL). The mixture was heated under reflux conditions for 30 min. After cooling, NaOH was removed by filtration, and the solvents were evaporated. The compounds were separated by column chromatography (heptane/CH_2Cl_2 70:30 then 20:80) to yield) **6** (0.66 g, 22 %) and **9** (1.54 g, 44 %). $R_f = 0.33$ (heptane/CH_2Cl_2 20:80); ^1H NMR (200.13 MHz, $CDCl_3$): $\delta = 7.61$ (d, $J = 7.6$ Hz, 2H), 7.47 (d, $J = 7.6$ Hz, 1H), 7.45 (m, 1H), 7.40 (d, $J = 7.6$ Hz, 1H), 7.38 (s, 1H), 3.15 (s, 1H), 2.04 (s, 1H), 1.94 (m, 4H), 1.65 (s, 6H), 1.07 (m, 4H), 0.66 (t, $J = 7.2$ Hz, 6H), 0.52 ppm (m, 4H); ^{13}C NMR (50.32 MHz, $CDCl_3$): $\delta =$ 150.92, 150.86, 141.0, 140.4, 131.2, 130.7, 126.4, 126.0, 121.5, 120.6, 119.9, 119.8, 94.0, 84.5, 82.9, 77.3, 65.7, 55.0, 40.1, 31.5, 25.7, 22.9, 13.7 ppm; HRMS (EI): m/z calcd for $C_{28}H_{32}O$ [$M^{+\bullet}$]: 384.2453; found: 384.2448; elemental analysis calcd (%) for $C_{28}H_{32}O$ (384.56): C 87.45, H 8.39; found: C 87.02, H 8.51.

Compound 10a: Air was removed from a solution of **9** (1.304 g, 3.39 mmol) and **7**[11] (1.71 g, 4.41 mmol) in toluene/Et_3N (5:1, 10.8 mL) by blowing argon for 20 min. Then CuI (12.9 mg, 0.068 mmol) and $[Pd(PPh_3)_2Cl_2]$ (48 mg, 0.068 mmol) were added, and deaeration was continued for 10 min. Thereafter the mixture was stirred at 40 °C for 3.5 h. The solvents were removed under reduced pressure, and the crude product was purified by column chromatography (heptane/CH_2Cl_2 75:25 then 30:70) to yield **10a** (817 mg, 37 %). $R_f = 0.37$ (heptane/CH_2Cl_2 30:70); ^1H NMR (200.13 MHz, $CDCl_3$): $\delta = 7.61$ (d, $J = 8.5$ Hz, 1H), 7.60 (d, $J =$ 8.5 Hz, 1H), 7.47 (d, $J = 8.5$ Hz, 1H), 7.45 (m, 1H), 7.39 (d, $J = 8.5$ Hz, 1H), 7.39 and 6.58 (AA′XX′, J(A,X) = 9.1 Hz, 4H), 7.37 (m, 1H), 3.28 (m, 4H), 2.08 (s, 1H), 1.95 (m, 4H), 1.66 (s, 6H), 1.65–1.52 (m, 4H), 1.32 (m, 12H), 1.08 (m, 4H), 0.90 (m, 6H), 0.67 (t, $J = 7.2$ Hz, 6H), 0.56 ppm (m, 4H); ^{13}C NMR (50.32 MHz, $CDCl_3$): $\delta = 150.8$ (2C), 147.9, 140.9, 139.6, 132.8, 130.7, 130.3, 125.9, 125.4, 123.0, 120.9, 119.8, 119.6, 111.1, 108.6, 93.7, 91.3, 88.0, 83.0, 65.6, 55.0, 50.9, 40.2, 31.6, 31.5, 27.1, 26.7, 25.8, 23.0, 22.6, 14.0, 13.8 ppm; HRMS (ES^+): m/z calcd for $C_{46}H_{62}NO$ [M+H]$^+$: 644.4831; found: 644.4832; elemental analysis calcd (%) for $C_{46}H_{61}NO$ (644.00): C 85.79, H 9.55, N 2.17; found: C 86.06, H 9.57, N 2.07.

Compound 10b: Solid KOH (0.07 g) was added to a solution of **10a** (0.798 g, 1.24 mmol) in toluene/*i*PrOH (6:1, 8.75 mL). The mixture was heated under reflux conditions for 1 h. After cooling, KOH was removed by filtration and the solvents were evaporated. The crude product was purified by column chromatography (heptane/CH_2Cl_2 90:10) to yield **10b** (0.632 g, 87 %). $R_f = 0.19$ (heptane/CH_2Cl_2 90:10); ^1H NMR (200.13 MHz, $CDCl_3$): $\delta = 7.63$ (d, $J = 8.5$ Hz, 1H), 7.62 (d, $J = 8.5$ Hz, 1H), 7.47 (d, $J =$ 8.5 Hz, 2H), 7.46 (m, 2H), 7.39 and 6.58 (AA′XX′, J(A,X) = 8.8 Hz, 4H), 3.28 (m, 4H), 3.14 (s, 1H), 1.96 (m, 4H), 1.60 (m, 4H), 1.32 (m, 12H), 1.08 (m, 4H), 0.90 (m, 6H), 0.67 (t, $J = 7.3$ Hz, 6H), 0.57 ppm (m, 4H); ^{13}C NMR (50.32 MHz, $CDCl_3$): $\delta = 150.91$, 150.85, 147.9, 141.4, 139.5, 132.8, 131.1, 130.3, 126.4, 125.5, 123.3, 120.3, 119.9, 119.6, 111.1, 108.6, 91.4, 88.0, 84.6, 77.1, 55.0, 50.9, 40.1, 31.7, 27.1, 26.8, 25.8, 23.0, 22.6, 14.0, 13.8 ppm; HRMS (ES^+): m/z calcd for $C_{43}H_{56}N$ [M+H]$^+$: 586.4413; found: 586.4411; elemental analysis calcd (%) for $C_{43}H_{55}N$ (585.92): C 88.15, H 9.46, N 2.39; found: C 87.89, H 9.59, N 2.40.

Compound 11a: Air was removed from a solution of **7**[11] (4.00 g, 10.33 mmol) in toluene/Et_3N (4:1, 75 mL) by blowing argon for 20 min. Then CuI (59.4 mg, 0.306 mmol), $[Pd(PPh_3)_2Cl_2]$ (216 mg, 0.306 mmol), and ethynyltrimethylsilane (3.25 mL, 2.25 g, 15.5 mmol) were added, and deaeration was continued for 5 min. Thereafter the mixture was stirred at 40 °C for 18 h. The solvents were removed under reduced pressure, and the crude product was purified by column chromatography (heptane/CH_2Cl_2 95:5 then 90:10) to yield **11a** (3.317 g, 90 %). $R_f = 0.50$ (heptane/CH_2Cl_2 90:10); ^1H NMR (200.13 MHz, $CDCl_3$): $\delta = 7.32$ and 6.54 (AA′XX′, J(A,X) = 8.9 Hz, 4H), 3.29 (m, 4H), 1.60 (m, 4H), 1.32 (m, 12H), 0.90 (m, 6H), 0.25 ppm (s, 9H); ^{13}C NMR (50.32 MHz, $CDCl_3$): $\delta = 148.6$, 133.4, 111.4, 108.7, 107.2, 91.0, 51.3, 32.1, 27.5, 27.1, 23.1, 14.2,

0.3 ppm; HRMS (EI): m/z calcd for $C_{23}H_{39}NSi$ [M^+]: 357.2852; found: 357.2857.

Compound 15a: A solution of **8** (1.93 g, 5.04 mmol) and 4-dimethylaminopyridine (DMAP; 0.61 g, 0.50 mmol) in CH_2Cl_2 (95 mL) was cooled at 0 °C, then Et_3N (1 mL) and CH_3COCl (0.54 mL, 7.56 mmol) were added dropwise. The mixture was stirred at 20 °C for 14 h. After addition of water, extraction with CH_2Cl_2, and drying (Na_2SO_4), the solvent was removed under reduced pressure. The residue was purified by column chromatography (heptane/CH_2Cl_2 50:50 then 40:60) to yield **15a** (1.63 g, 76 %). R_f = 0.25 (heptane/CH_2Cl_2 50:50); ^{1}H NMR (200.13 MHz, $CDCl_3$): δ = 7.47 and 6.52 (AA′XX′, J(A,X) = 9.0 Hz, 4H), 7.01 and 6.88 (AA′BB′, J(A,B) = 9.1 Hz, 4H), 4.10 (t, J = 6.0 Hz, 2H), 3.65 (t, J = 6.0 Hz, 2H), 3.43 (q, J = 7.0 Hz, 2H), 2.21 (s, 3H), 1.17 ppm (t, J = 7.0 Hz, 3H); ^{13}C NMR (50.32 MHz, $CDCl_3$): δ = 169.8, 156.2, 147.0, 144.3, 137.8, 122.3, 115.0, 114.1, 76.5, 65.6, 49.5, 45.5, 21.1, 12.0 ppm.

Compound 15b: Air was removed from a solution of **15a** (1.647 g, 3.87 mmol) in toluene/Et_3N (4:1, 16 mL) by blowing argon for 20 min. Then CuI (14.8 mg, 0.078 mmol), [Pd(PPh_3)$_2$Cl$_2$] (54.4 mg, 0.078 mmol), and ethynyltrimethylsilane (0.82 mL, 0.570 g, 5.805 mmol) were added, and deaeration was continued for 5 min. Thereafter the mixture was stirred at 40 °C for 15 h. The solvents were removed under reduced pressure, and the crude product was purified by column chromatography (heptane/CH_2Cl_2 50:50 then 40:60) to yield **15b** (1.246 g, 81 %). R_f = 0.28 (heptane/CH_2Cl_2 60:40); ^{1}H NMR (200.13 MHz, $CDCl_3$): δ = 7.32 and 6.60 (AA′XX′, J(A,X) = 9.0 Hz, 4H), 6.98 and 6.84 (AA′BB′, J(A,B) = 9.1 Hz, 4H), 4.08 (t, J = 6.0 Hz, 2H), 3.71 (t, J = 6.0 Hz, 2H), 3.47 (q, J = 7.0 Hz, 2H), 2.27 (s, 3H), 1.18 (t, J = 7.0 Hz, 3H), 0.22 ppm (s, 9H); ^{13}C NMR (50.32 MHz, $CDCl_3$): δ = 169.4, 156.0, 147.2, 144.1, 133.1, 122.1, 114.7, 111.0, 109.4, 106.4, 90.9, 65.5, 49.2, 45.3, 20.7, 11.9, 0.0 ppm; HRMS (EI): m/z calcd for $C_{23}H_{29}NO_3Si$ [M^+]: 395.1917; found: 395.1924.

Compound 15c: TBAF (1 M in THF, 0.97 mL, 0.97 mmol) was added to a solution of **15b** (219 mg, 0.962 mmol) in THF (10 mL), and the mixture was stirred at 20 °C for 15 min. After addition of $CaCl_2$, the solvent was removed under reduced pressure, and the residue was purified by column chromatography (heptane/CH_2Cl_2 30:70) to yield **15c** (140 mg, 45 %). R_f = 0.20 (heptane/CH_2Cl_2 30:70); ^{1}H NMR (200.13 MHz, $CDCl_3$): δ = 7.37 and 6.64 (AA′XX′, J(A,X) = 8.8 Hz, 4H), 7.00 and 6.87 (AA′BB′, J(A,B) = 9.4 Hz, 4H), 4.09 (t, J = 6.0 Hz, 2H), 3.72 (t, J = 6.0 Hz, 2H), 3.48 (q, J = 7.0 Hz, 2H), 2.99 (s, 1H), 2.28 (s, 3H), 1.20 ppm (t, J = 7.0 Hz, 3H); ^{13}C NMR (50.32 MHz, $CDCl_3$): δ = 169.7, 156.2, 147.6, 144.3, 133.4, 122.3, 114.9, 111.2, 108.4, 84.7, 74.8, 65.6, 49.4, 45.5, 21.0, 12.1 ppm.

Compound 16: Air was removed from a solution of **5a**[10] (4.267 g, 8.047 mmol) and **15b** (1.06 g, 2.681 mmol) in toluene/Et_3N (5:1, 13 mL) by blowing argon for 20 min. Then CuI (10.3 mg, 0.054 mmol), [Pd(PPh_3)$_2$Cl$_2$] (37.9 mg, 0.054 mmol), and TBAF (1 M in THF, 2.8 mL, 2.8 mmol) were added, and the mixture was stirred at 40 °C for 15 h. After evaporation of the solvents, the residue was purified by column chromatography (heptane/CH_2Cl_2 80:20, then 70:30) to yield **16** (1.052 g, 54 %). R_f = 0.48 (heptane/CH_2Cl_2 80:20); ^{1}H NMR (200.13 MHz, $CDCl_3$): δ = 7.73 (s, 1H), 7.70 (d, J = 7.6 Hz, 1H), 7.66 (d, J = 8.0 Hz, 1H), 7.53 (d, J = 8.0 Hz, 1H), 7.51 (s, 1H), 7.49 and 6.74 (AA′XX′, J(A,X) = 8.8 Hz, 4H), 7.46 (d, J = 7.6 Hz, 1H), 7.05 and 6.92 (AA′BB′, J(A,B) = 9.0 Hz, 4H), 4.16 (t, J = 5.9 Hz, 2H), 3.80 (t, J = 5.9 Hz, 2H), 3.55 (q, J = 7.1 Hz, 2H), 2.32 (s, 3H), 1.93 (m, 4H), 1.23 (t, J = 7.1 Hz, 3H), 1.09 (m, 4H), 0.68 (t, J = 7.0 Hz, 6H), 0.57 ppm (m, 4H); ^{13}C NMR (50.32 MHz, $CDCl_3$): δ = 169.7, 156.2, 153.3, 150.0, 147.3, 144.4, 140.2, 139.5, 135.9, 133.0, 132.0, 130.4, 125.5, 123.1, 122.9, 121.5, 119.7, 115.0, 111.4, 109.8, 92.7, 91.0, 88.3, 65.7, 55.2, 49.5, 45.6, 40.1, 25.8, 23.0, 21.0, 13.8, 12.2 ppm.

Compound 2: Air was removed from a solution of **16** (0.952 g, 1.31 mmol) and **11a** (0.546 g, 1.574 mmol) in toluene/Et_3N (5:1, 8.5 mL) by blowing argon for 20 min. Then CuI (5.2 mg, 0.027 mmol), [Pd(PPh_3)$_2$Cl$_2$] (18.9 mg, 0.027 mmol), and TBAF (1 M in THF, 1.7 mL, 1.7 mmol) were added, and the mixture was stirred at 40 °C for 15 h. After evaporation of the solvents, the residue was purified by column chromatography (heptane/CH_2Cl_2 60:40 then 50:50) to yield **17** (0.868 g, 75 %). R_f = 0.39 (heptane/CH_2Cl_2 50:50); ^{1}H NMR (200.13 MHz, $CDCl_3$): δ = 7.62 (d, J = 7.8 Hz, 2H), 7.47 (d, J = 7.5 Hz, 2H), 7.45 (m, 2H), 7.43 and 6.68 (AA′XX′, J(A,X) = 8.6 Hz, 4H), 7.39 and 6.58 (AA′XX′, J(A,X) = 8.5 Hz, 4H), 6.99 and 6.87 (AA′BB′, J(A,B) = 9.1 Hz, 4H), 4.11 (t, J = 6.4 Hz, 2H), 3.75 (t, J = 6.4 Hz, 2H), 3.50 (q, J = 6.9 Hz, 2H), 3.28 (m, 4H), 2.27 (s, 3H), 1.97 (m, 4H), 1.59 (m, 4H), 1.32 (m, 12H), 1.22 (t, J = 6.9 Hz, 3H), 1.09 (m, 4H), 0.88 (m, 6H), 0.67 (t, J = 7.2 Hz, 6H), 0.59 ppm (m, 4H). Aqueous NaOH (8.5 mL, 0.5 M) was added to a solution of **17** (0.852 g, 0.965 mmol) in THF/EtOH (2:1, 54 mL). The mixture was stirred at 20 °C for 15 min, then aqueous HCl (9 mL, 0.5 M) was added. After the addition of water, extraction with CH_2Cl_2, and drying ($MgSO_4$), the solvents were removed under reduced pressure. The crude product was purified by column chromatography (heptane/CH_2Cl_2 20:80 then 10:90) to yield **2** (739 mg, 91 %). R_f = 0.31 (heptane/CH_2Cl_2 20:80); ^{1}H NMR (200.13 MHz, $CDCl_3$): δ = 7.62 (d, J = 8.4 Hz, 2H), 7.47 (d, J = 8.4 Hz, 2H), 7.45 (m, 2H), 7.43 and 6.72 (AA′XX′, J(A,X) = 9.1 Hz, 4H), 7.39 and 6.58 (AA′XX′, J(A,X) = 8.9 Hz, 4H), 6.76 (m, 4H), 4.58 (s, 1H), 4.07 (t, J = 6.1 Hz, 2H), 3.72 (t, J = 6.1 Hz, 2H), 3.50 (q, J = 6.9 Hz, 2H), 3.28 (m, 4H), 1.97 (m, 4H), 1.60 (m, 4H), 1.32 (m, 12H), 1.21 (t, J = 6.9 Hz, 3H), 1.09 (m, 4H), 0.90 (m, 6H), 0.67 (t, J = 7.2 Hz, 6H), 0.59 ppm (m, 4H); ^{13}C NMR (50.32 MHz, $CDCl_3$): δ = 152.6, 151.0, 150.9, 149.9, 147.9, 147.4, 140.1, 139.9, 132.9, 132.8, 130.3, 125.5, 122.7, 122.5, 119.7, 119.6, 116.1, 115.5, 111.4, 111.2, 109.8, 108.7, 91.2, 90.8, 88.4, 88.2, 66.0, 55.0, 50.9, 49.6, 45.5, 40.2, 31.7, 27.1, 26.8, 25.8, 23.0, 22.6, 14.0, 13.8, 12.2 ppm; HRMS (ES$^+$): m/z calcd for $C_{59}H_{73}N_2O_2$ [M+H]$^+$: 841.5672; found: 841.5660; elemental analysis calcd (%) for $C_{59}H_{72}N_2O_2$ (841.24): C 84.24, H 8.63, N 3.33; found: C 83.84, H 8.52, N 3.38.

Compound 18: Air was removed from a solution of **15b** (0.232 g, 0.588 mmol) and **5a**[10] (0.130 g, 0.245 mmol) in toluene/Et_3N (4:1, 3.8 mL) by blowing argon for 20 min. Then CuI (2.3 mg, 0.012 mmol), [Pd(PPh_3)$_2$Cl$_2$] (8.6 mg, 0.012 mmol), and TBAF (1 M in THF, 0.6 mL, 0.6 mmol) were added, and deaeration was continued for 10 min. Thereafter the mixture was stirred at 40 °C for 16 h. The solvents were removed under reduced pressure, and the crude product was purified by column chromatography (heptane/CH_2Cl_2 40:60, then 30:70) to yield **18** (0.169 g, 76 %). R_f = 0.58 (CH_2Cl_2); ^{1}H NMR (200.13 MHz, $CDCl_3$): δ = 7.63 (d, J = 7.8 Hz, 2H), 7.48 (d, J = 7.8 Hz, 2H), 7.46 (m, 2H), 7.43 and 6.68 (AA′XX′, J(A,X) = 8.9 Hz, 8H), 6.99 and 6.88 (AA′BB′, J(A,B) = 9.1 Hz, 8H), 4.11 (t, J = 6.0 Hz, 4H), 3.75 (t, J = 6.0 Hz, 4H), 3.51 (q, J = 7.0 Hz, 4H), 2.28 (s, 6H), 1.97 (m, 4H), 1.22 (t, J = 7.0 Hz, 6H), 1.09 (m, 4H), 0.67 (t, J = 7.3 Hz, 6H), 0.58 ppm (m, 4H); ^{13}C NMR (50.32 MHz, $CDCl_3$): δ = 166.3, 156.3, 150.9, 147.3, 144.3, 140.1, 133.0, 130.3, 125.5, 122.5, 122.4, 119.7, 115.0, 111.3, 109.8, 90.7, 88.4, 65.7, 55.0, 49.5, 45.6, 40.3, 25.8, 23.0, 21.0, 13.9, 12.3 ppm; elemental analysis calcd (%) for $C_{61}H_{64}N_2O_6$ (921.19): C 79.54, H 7.00, N 3.04; found: C 79.20, H 7.08, N 2.92.

Compound 3: Aqueous NaOH (1.5 mL, 0.5 M) was added to a solution of **18** (80 mg, 0.087 mmol) in THF/EtOH (2:1, 4.5 mL). The mixture was stirred at 20 °C for 25 min, then aqueous HCl (7.5 mL, 0.1 M) was added. After addition of water, extraction with CH_2Cl_2, and drying (Na_2SO_4), the solvents were removed under reduced pressure. The residue was purified by column chromatography (CH_2Cl_2, then CH_2Cl_2/AcOEt 98:2) to yield **3** (72 mg, 98 %). R_f = 0.41 (CH_2Cl_2/AcOEt 95:5); ^{1}H NMR (200.13 MHz, $CDCl_3$): δ = 7.62 (d, J = 8.1 Hz, 2H), 7.47 (d, J = 8.1 Hz, 2H), 7.46 (m, 2H), 7.43 and 6.68 (AA′XX′, J(A,X) = 8.8 Hz, 8H), 6.76 (m, 8H), 4.58 (s, 2H), 4.07 (t, J = 6.0 Hz, 4H), 3.72 (t, J = 6.0 Hz, 4H), 3.50 (q, J = 6.9 Hz, 4H), 1.97 (m, 4H), 1.22 (t, J = 6.9 Hz, 6H), 1.09 (m, 4H), 0.67 (t, J = 7.3 Hz, 6H), 0.59 ppm (m, 4H); ^{13}C NMR (50.32 MHz, $CDCl_3$): δ = 152.7, 150.9, 149.7, 147.4, 140.1, 132.9, 130.3, 125.5, 122.5, 119.7, 116.0, 115.5, 111.4, 109.8, 90.8, 88.4, 66.0, 55.0, 49.6, 45.6, 40.3, 25.8, 23.0, 13.8, 12.2 ppm; HRMS (ES$^+$): m/z calcd for $C_{57}H_{60}N_2O_4Na$ [M+Na]$^+$: 859.4451; found: 859.4407; m/z calcd for $C_{57}H_{60}N_2O_4K$ [M+K]$^+$: 875.4190; found: 875.4149.

Compound 1: Air was removed from a solution of **11a** (0.410 g, 1.146 mmol) and **5a** (0.303 g, 0.571 mmol) in THF/Et_3N (4:1, 5.5 mL) by blowing argon for 20 min. Then CuI (4.9 mg, 0.026 mmol), [Pd(PPh_3)$_2$Cl$_2$] (18 mg, 0.026 mmol), and TBAF (1 M in THF, 1.8 mL) were added, and deaeration was continued for 10 min. Thereafter the mixture was stirred at 50 °C for 16 h. The solvents were removed under reduced pressure, and the crude product was purified by column chromatography (heptane/CH_2Cl_2 95:5, then 90:10) to yield **1** (286 mg, 59 %). R_f = 0.29 (heptane/

CH_2Cl_2 90:10); ^1H NMR (300.13 MHz, $CDCl_3$): $\delta = 7.62$ (d, $J = 7.8$ Hz, 2H), 7.47 (dd, $J = 7.8$ Hz, 1.5 Hz, 2H), 7.46 (m, 2H), 7.40 and 6.58 (AA′XX′, J(A,X) = 9.0 Hz, 8H), 3.28 (m, 8H), 1.97 (m, 4H), 1.59 (m, 8H), 1.32 (m, 24H), 1.09 (m, 4H), 0.91 (t, $J = 6.8$ Hz, 12H), 0.67 (t, $J =$ 7.4 Hz, 6H), 0.59 ppm (m, 4H); ^{13}C NMR (50.32 MHz, $CDCl_3$): $\delta = 151.3$, 148.3, 140.4, 133.2, 130.7, 125.9, 123.1, 120.1, 111.6, 109.2, 91.5, 88.6, 55.4, 51.4, 40.7, 32.1, 27.6, 27.2, 26.3, 23.5, 23.1, 14.2 ppm; HRMS (ES^+): m/z calcd for $C_{61}H_{85}N_2$ $[M+H]^+$: 845.6713; found: 845.6716; elemental analysis calcd (%) for $C_{61}H_{84}N_2$ (845.33): C 86.67, H 10.02, N 3.31; found: C 86.40, H 10.16, N 3.41.

Photophysical methods: All photophysical properties were analyzed with freshly prepared air-equilibrated solutions at room temperature (298 K). UV/Vis absorption spectra were recorded using a Jasco V-570 spectrophotometer. Steady-state and time-resolved fluorescence measurements were performed on dilute solutions (approximately 10^{-6} M, optical density < 0.1) contained in standard 1 cm quartz cuvettes using an Edinburgh Instruments (FLS920) spectrometer in photon-counting mode. Fully corrected emission spectra were obtained for each compound at $\lambda_{ex} = \lambda_{max}^{abs}$ with an optical density at $\lambda_{ex} \leq 0.1$ to minimize internal absorption. Fluorescence quantum yields were measured according to literature procedures.[24] Fluorescence lifetimes were measured by time-correlated single-photon counting (TCSPC) by using the same FLS 920 fluorimeter. Excitation was achieved by using a hydrogen-filled nanosecond flashlamp (repetition rate 40 kHz). The instrument response (full width at half-maximum (FWHM) approximately 1 ns) was determined by measuring the light scattered by a Ludox suspension. The TCSPC traces were analyzed by standard iterative reconvolution methods implemented in the software of the fluorimeter. All compounds displayed strictly monoexponential fluorescence decays ($\chi^2 < 1.1$).

Two-photon absorption (TPA): Two-photon absorption measurements were conducted by investigating the two-photon excited fluorescence (TPEF) of the fluorophores in THF at room temperature on air-equilibrated solutions (10^{-4} M) according to the experimental protocol established by Xu and Webb.[5] This protocol avoids contributions from excited-state absorption that are known to result in largely overestimated TPA cross-sections. To span the 700–980 nm range, a Nd:YLF-pumped Ti:sapphire oscillator was used to generate 150 fs pulses at a 76 MHz rate. The excitation was focused into the cuvette through a microscope objective (10×; numerical aperture (NA): 0.25). The fluorescence was detected in epifluorescence mode by using a dichroic mirror (Chroma 675dcxru) and a barrier filter (Chroma e650sp-2p) by a compact CCD spectrometer module (BWTek BTC112E). Total fluorescence intensities were obtained by integrating the corrected emission spectra measured by this spectrometer. TPA cross-sections (σ_2) were determined from the two-photon excited fluorescence (TPEF) cross-sections ($\sigma_2\Phi$) and the fluorescence emission quantum yield (Φ). TPEF cross-sections were measured relative to fluorescein in 0.01 M aqueous NaOH for 715–980 nm[5,25] and the appropriate solvent-related refractive index corrections.[26] Data points between 700 and 715 nm were corrected according to the literature.[27] The quadratic dependence of the fluorescence intensity on the excitation power was checked for each sample and all wavelengths, thereby indicating that the measurements were carried out in intensity regimes in which saturation or photodegradation did not occur.

Acknowledgements

ANR PCV2007 (Biodendridot) is gratefully acknowledged for a fellowship to M.C. We thank Région Bretagne for a fellowship to C.R. and CNRS for a grant to T.R.K. M.B.D gratefully acknowledges financial support from the Conseil Régional d'Aquitaine (Chaire d'excellence grant). We wish to thank J. Robert and H. Simon for assistance in the synthesis.

[1] a) W. Denk, J. H. Strickler, W. W. Webb, *Science* **1990**, *248*, 73–76; b) C. Xu, W. Zipfel, J. B. Shear, R. M. Williams, W. W. Webb, *Proc. Natl. Acad. Sci. USA* **1996**, *93*, 10763–10768; c) H. M. Kim, B. R. Cho, *Acc. Chem. Res.* **2009**, *42*, 863–872; d) H. M. Kim, B. R. Cho, *Chem. Asian J.* **2011**, *6*, 58–69; e) S. Sumalekshmy, C. J. Fahrni, *Chem. Mater.* **2011**, *23*, 483–500; f) S. Yao, K. D. Belfield, *Eur. J. Org. Chem.* **2012**, *2012*, 3199–3217.

[2] a) J. D. Bhawalkar, N. D. Kumar, C. F. Zhao, P. N. Prasad, *J. Clin. Laser Med. Surg.* **1997**, *15*, 201–204; b) P. K. Frederiksen, M. Jørgensen, P. R. Ogilby, *J. Am. Chem. Soc.* **2001**, *123*, 1215–1221; c) S. Kim, T. Y. Ohulchanskyy, H. E. Pudavar, R. K. Pandey, P. N. Prasad, *J. Am. Chem. Soc.* **2007**, *129*, 2669–2675; d) J. R. Starkey, A. K. Rebane, M. A. Drobizhev, F. Meng, A. Gong, A. Elliott, K. McInnerney, C. W. Spangler, *Clin. Cancer Res.* **2008**, *14*, 6564–6573; e) H. A. Collins, M. Khurana, E. H. Moriyama, A. Mariampillai, E. Dahlstedt, M. Balaz, M. K. Kuimova, M. Drobizhev, X. D. YangVictor, D. Phillips, A. Rebane, B. C. Wilson, H. L. Anderson, *Nat. Photonics* **2008**, *2*, 420.

[3] a) T. Furuta, S. S. H. Wang, J. L. Dantzker, T. M. Dore, W. J. Bybee, E. M. Callaway, W. Denk, R. Y. Tsien, *Proc. Natl. Acad. Sci. USA* **1999**, *96*, 1193–1200; b) M. Matsuzaki, G. C. R. Ellis-Davies, T. Nemoto, Y. Miyashita, M. Iino, H. Kasai, *Nature Neuroscience* **2001**, *4*, 1086–1092; c) A. Momotake, N. Lindegger, E. Niggli, R. J. Barsotti, G. C. R. Ellis-Davies, *Nature Methods* **2006**, *3*, 35–40; d) A.-C. Robin, S. Gmouh, O. Mongin, V. Jouikov, M. H. V. Werts, C. Gautier, A. Slama-Schwok, M. Blanchard-Desce, *Chem. Commun.* **2007**, 1334–1336; e) E. Beaumont, J.-C. Lambry, A.-C. Robin, P. Martasek, M. Blanchard-Desce, A. Slama-Schwok, *ChemPhysChem* **2008**, *9*, 2325–2331.

[4] W. R. Zipfel, R. M. Williams, R. Christie, A. Y. Nikitin, B. T. Hyman, W. W. Webb, *Proc. Natl. Acad. Sci. USA* **2003**, *100*, 7075–7080.

[5] C. Xu, W. W. Webb, *J. Opt. Soc. Am. B* **1996**, *13*, 481–491.

[6] a) F. Terenziani, C. Katan, E. Badaeva, S. Tretiak, M. Blanchard-Desce, *Adv. Mater.* **2008**, *20*, 4641–4678; b) G. S. He, L.-S. Tan, Q. Zheng, P. N. Prasad, *Chem. Rev.* **2008**, *108*, 1245–1330; c) H. M. Kim, B. R. Cho, *Chem. Commun.* **2009**, 153–164; d) M. Pawlicki, H. A. Collins, R. G. Denning, H. L. Anderson, *Angew. Chem.* **2009**, *121*, 3292–3316; *Angew. Chem. Int. Ed.* **2009**, *48*, 3244–3266.

[7] a) O. Mongin, T. R. Krishna, M. H. V. Werts, A.-M. Caminade, J.-P. Majoral, M. Blanchard-Desce, *Chem. Commun.* **2006**, 915–917; b) M. Blanchard-Desce, M. Werts, O. Mongin, J.-P. Majoral, A.-M. Caminade, R. K. Thatavarthy, PCT Int. Appl., WO, **2007**, 2007080176; c) O. Mongin, C. Rouxel, A.-C. Robin, A. Pla-Quintana, T. R. Krishna, G. Recher, F. Tiaho, A.-M. Caminade, J.-P. Majoral, M. Blanchard-Desce, *Proc. SPIE-Int. Soc. Opt. Eng.* **2008**, *7040*, 704006, 1–12; d) O. Mongin, C. Rouxel, J.-M. Vabre, Y. Mir, A. Pla-Quintana, Y. Wei, A.-M. Caminade, J. P. Majoral, M. Blanchard-Desce, *Proc. SPIE* **2009**, *7403*, 740303.

[8] T. R. Krishna, M. Parent, M. H. V. Werts, L. Moreaux, S. Gmouh, S. Charpak, A.-M. Caminade, J.-P. Majoral, M. Blanchard-Desce, *Angew. Chem.* **2006**, *118*, 4761–4764; *Angew. Chem. Int. Ed.* **2006**, *45*, 4645–4648.

[9] a) L. Ventelon, S. Charier, L. Moreaux, J. Mertz, M. Blanchard-Desce, *Angew. Chem.* **2001**, *113*, 2156–2159; *Angew. Chem. Int. Ed.* **2001**, *40*, 2098–2101; b) M. H. V. Werts, S. Gmouh, O. Mongin, T. Pons, M. Blanchard-Desce, *J. Am. Chem. Soc.* **2004**, *126*, 16294–16295; c) O. Mongin, L. Porrès, M. Charlot, C. Katan, M. Blanchard-Desce, *Chem. Eur. J.* **2007**, *13*, 1481–1498.

[10] F. Li, Z. Chen, W. Wei, H. Cao, Q. Gong, F. Teng, L. Qian, Y. Wang, *J. Phys. D: Appl. Phys.* **2004**, *37*, 1613–1616.

[11] C. Käpplinger, R. Beckert, *Synthesis* **2002**, 1843–1850.

[12] B. Traber, J. J. Wolff, F. Rominger, T. Oeser, R. Gleiter, M. Goebel, R. Wortmann, *Chem. Eur. J.* **2004**, *10*, 1227–1238.

[13] T. A. Cross, M. C. Davis, *Synth. Commun.* **2008**, *38*, 499–516.

[14] N. Launay, A.-M. Caminade, R. Lahana, J.-P. Majoral, *Angew. Chem.* **1994**, *106*, 1682; *Angew. Chem. Int. Ed. Engl.* **1994**, *33*, 1589.

[15] C. Loup, M.-A. Zanta, A.-M. Caminade, J.-P. Majoral, B. Meunier, *Chem. Eur. J.* **1999**, *5*, 3644–3650.

[16] O. Mongin, A. Pla-Quintana, F. Terenziani, D. Drouin, C. Le Droumaguet, A.-M. Caminade, J.-P. Majoral, M. Blanchard-Desce, *New J. Chem.* **2007**, *31*, 1354–1367.

[17] D. A. McQuarrie, J. D. Simon, *Physical Chemistry: A Molecular Approach*, University Science Books, Sausalito, **1997**.
[18] F. Terenziani, A. Painelli, C. Katan, M. Charlot, M. Blanchard-Desce, *J. Am. Chem. Soc.* **2006**, *128*, 15742–15755.
[19] a) E. Lippert, *Z. Naturforsch. A* **1955**, *10*, 541–545; b) N. Mataga, Y. Kaifu, M. Koizumi, *Bull. Chem. Soc. Jpn.* **1955**, *28*, 690–691.
[20] a) C. Katan, M. Charlot, O. Mongin, C. Le Droumaguet, V. Jouikov, F. Terenziani, E. Badaeva, S. Tretiak, M. Blanchard-Desce, *J. Phys. Chem. B* **2010**, *114*, 3152–3169; b) S. Amthor, C. Lambert, S. Dummler, I. Fischer, J. Schelter, *J. Phys. Chem. A* **2006**, *110*, 5204–5214.
[21] P. Suppan, *J. Photochem. Photobiol. A* **1990**, *50*, 293–330.
[22] J. R. Lakowicz, *Principles of Fluorescence Spectroscopy*, Kluwer Academic/Plenum Publishers, New York, **1999**.
[23] C. Rouxel, M. Charlot, Y. Mir, C. Frochot, O. Mongin, M. Blanchard-Desce, *New J. Chem.* **2011**, *35*, 1771–1780.
[24] a) D. F. Eaton, *Pure Appl. Chem.* **1988**, *60*, 1107–1114; b) J. N. Demas, G. A. Crosby, *J. Phys. Chem.* **1971**, *75*, 991–1024.
[25] M. A. Albota, C. Xu, W. W. Webb, *Appl. Opt.* **1998**, *37*, 7352–7356.
[26] M. H. V. Werts, N. Nerambourg, D. Pélégry, Y. Le Grand, M. Blanchard-Desce, *Photochem. Photobiol. Sci.* **2005**, *4*, 531–538.
[27] C. Katan, S. Tretiak, M. H. V. Werts, A. J. Bain, R. J. Marsh, N. Leonczek, N. Nicolaou, E. Badaeva, O. Mongin, M. Blanchard-Desce, *J. Phys. Chem. B* **2007**, *111*, 9468–9483.

Received: August 7, 2012
Published online: November 8, 2012

